

Electronic structure, magnetic and Fermi surface calculations of heavy-fermions superconductors compounds based on Nb₃Sn

Badis BENDJEMIL^{1,2,*}

¹⁾ LEREc, Department of Physics, University of Annaba, 23000 Annaba, Algeria.

²⁾ University of Guelma, 24000 Guelma, Algeria.

Abstract

We report a theoretical investigation of the electronic structures and Fermi surface of the heavy-fermion superconductors Nb₃Sn. The electronic structures are investigated ab-initio on the basis of full-potential local orbital minimum-basis band-structure calculations (FPLO), adopting both the scalar- and fully relativistic formulations within the framework of the local spin-density approximation (LSDA). The possibility of a partial _{4d} localization occurring for compounds is discussed. The electronic structures of the Nb₃Sn compounds are computed to be rather similar to the literature. Our total-energy calculations predict paramagnetic and ferromagnetic order to be favorable for Nb₃Sn materials, which is, however, observed experimentally. Also, the calculated magnetic moment is 0.35 μ_B. Furthermore, the theoretical Fermi surfaces topology and the possible origins of the superconductivity are discussed. The Bardeen, Cooper and Schreiffer (BCS) energy gap and the Ginzburg-Landau (GL) parameter K for these compounds have been calculated from the Fermi velocity. We found strong indication suggesting the existence of a second superconducting (SC) gap in Nb₃Sn. In addition, the average superconductivity-gap at zero temperature is calculated for this compound. The knowledge of energy gap value gives important information on the coupling scenarios. Our results provide an explanation between the electronic structures, the Fermi surface (FS) topology and two-band model of the superconductivity.

Keywords: Fermi surface, Fermi velocity, Superconducting-gap, LSDA, FPLO.

1. Introduction

Since the discovery of the high-T_c cuprates, work on A₁₅ superconductors in the A₃B structure, with A a transition metal and B a sp-metal, has virtually ceased-this despite the many fundamental questions about these materials that remain open. One of them is Nb₃Sn which exhibits a great variety of phenomena such as the existence of two-gap superconductivity [1], the apparent controversy in different determinations of the specific heat [2] and the controversial origin of the superconducting coupling [3]. Several studies have

^{*}) Corresponding Author; Tel/Fax: 00 213 038 87 25 00; e-mail: Badis23@yahoo.fr.

shown that the specific heat of Nb_3Sn clues not varnish exponentially at low temperature below $T_c/4$ these studies were generally limited to zero field or were not sufficiently detailed, so be drawn. The use of high-resolution angle resolved photoemission spectroscopy (ARPES) directly observes the multiple (SC) gaps by resolving the σ and π bands.

In this paper, we reinvestigate the specific heat using the full potential nonorthogonal local-orbital minimum basis scheme. We present first ab-initio calculation, obtained Fermi surface using σ and π contribution clearly isolated from the surface band and Fermi sheets dependent of the (SC) gap. These results reveal the nature of multiple (SC) gap of Nb_3Sn . A_{15} materials display a fascinatingly rich variety unusual physical phenomenon. Among these are, e.g., strong-electron correlations, leading to heavy-fermion or Kondo insulating states, and exotic magnetic and orbital ordering. All theses phenomena are related to the peculiar behaviour of the Nb_3Sn $4d$ -electrons:

Varying one A_{15} structure material to another (V_3Si , V_3Ge , Nb_3G , Nb_3Al , Nb_3Ge ...), these may change their nature from being almost delocalised and bonding to localize and non-bonding. Cooper pairs are formed by Nb $4d$ -electrons pairing [4]. Nb_3Sn is well-known superconductor for years; another discovery has drawn worldwide attention: Superconductivity in Nb_3Sn based on the design of quadripolar magnets of the Broad High-Energy particle collider in NbTi in the reactor ITER-FEAT (Fusion plasma energy advanced Tokamak). Previously, no Sn-based superconductors were known, while most A_{15} superconductors exhibit T_c 's of less than 18 K.

2. Computation aspects

We performed band-structure calculations using both the scalar-relativistic and the fully relativistic versions of the FPLO method [5, 6]. In these calculations, the following basis sets were adopted for the valence states: Nb $4d_{5s}$ and Sn $4d_{5s}5p$ states were chosen as a minimum-basis set for the valence states. All lower lying states were treated as core states. The spatial extension of the basis orbital, controlled by a confining potential [7] $(r/r_0)^4$, was optimized to minimize the total energy. The self-consistent potentials were carried out on a k mesh of 20 k points in each direction of the Brillouin zone. The Wyckoff position of Nb and Sn are $(\frac{1}{4} 0 \frac{1}{2}), (0 0 0)$, respectively.

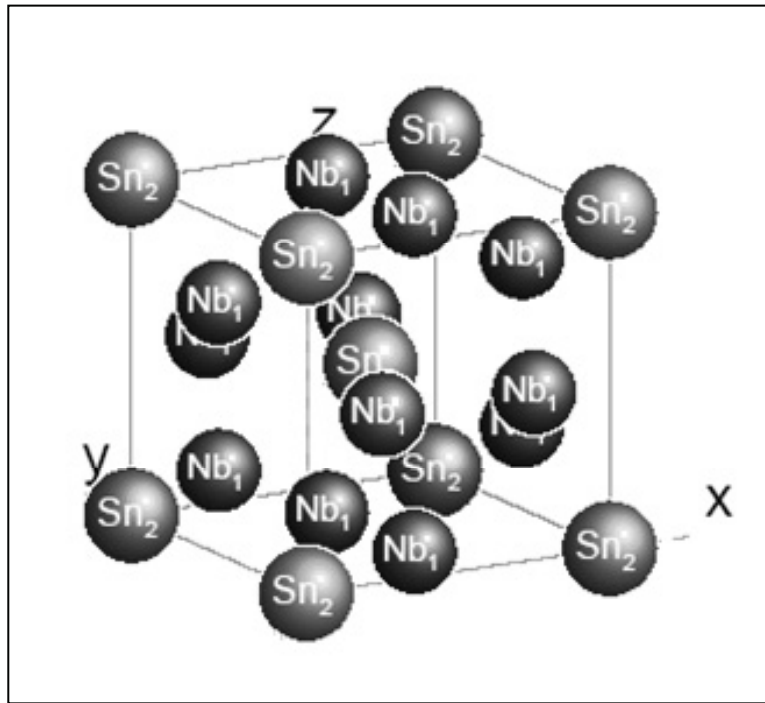
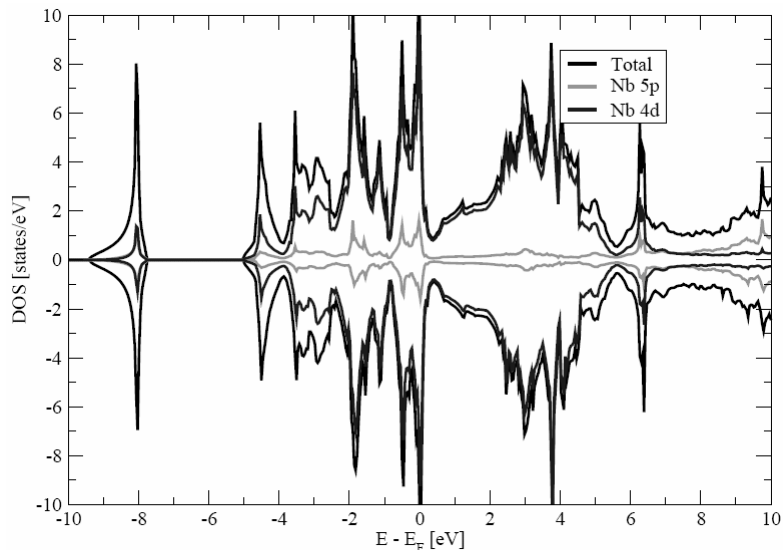
The compression parameters x_0 were optimized for each basis orbital separately by minimizing the total energy. For the site-centered potentials and densities we used expansions in spherical harmonics up to $l_{\max}=12$. The number of k points in the irreducible part of Brillouin zone was 636, but some pivotal calculations were made also with higher numbers of k points. The calculations were made also with 460 and up to 1666 k -points to resolve the density of states at E_F . The Perdew-Zunger [8] parameterization of the exchange-correlation potential in LSDA was used.

The dHvA cyclotron frequency F which is proportional to the Fermi surface cross section and the cyclotron mass m of the extremal orbits will be calculated numerically by discretizing the Fermi velocities on k points along the orbit and by a subsequent Romberg integration.

3. Results and Discussions

3(a) Electronic and magnetic calculation

The Nb_3Sn compound crystallize in the cubic and tetragonal structure ($\text{Pm}3n$ space group), with the lattice constants $a=5.2906 \text{ \AA}^\circ$ is shown in Figure 1.

Fig. 1: (Colour online) Crystal structure of Nb_3Sn Fig.2: (Colour online) Calculated total and partial density of states (DOS) of Nb_3Sn in the ferromagnetic phase, for the experimental lattice parameters. Note that the spin-projected partial DOS of only one paramagnetic type of atom is plotted, but with spin up and spin down DOS

In Figure 2 we show the calculated partial DOS (PDOS) of Nb_3Sn in the ferromagnetic phase (for the experimental lattice constants). The PDOS of the ferromagnetic phase is rather similar to that of the paramagnetic. The dominant contribution to the total DOS in the vicinity of E_F stems from the Nb_{4d} states. The Sn_{5p} states are rather smaller and delocalized and occur moderately deep below E_F , at a binding energy of 1–2.5 eV. The Nb_{4d} states are very dispersive, extending from -10 eV to above 10 eV. Near the Fermi energy the main hybridization occurring is that of Nb_{4d} and Sn_{5p} states. There is a large peak in the DOS close to E_F located at 0.5 eV. The peaks in the DOS near the Fermi energy are very sensitive to the Nb sublattice distortion (Fig.1) also (see [9, 10]). These results agree well with the calculation of Freericks et al. [11]. It should note that near the Fermi energy, the DOS is almost completely due to Nb. A striking difference in comparison to MgB_2 is the dominating

contribution of Nb_{4d} band to the total DOS at the Fermi energy, which contribute about 85 % of the total DOS; in MgB_2 the DOS at Fermi energy is dominated by B_{2p} states [12]. A strong hybridization between the Nb_{4d} and Sn_{5s} states is shown in Figure 3. Thus, the electrons at E_F have dominantly Nb_{4d} character, therefore it was concluded value of the density of states at the Fermi level $N(E_F)$ is much higher for Nb_3Sn , [$N(E_F)= 10 \text{ states/eV cell}$] than for MgB_2 [$N(E_F)= 0.71 \text{ states/eV cell}$] state occurs in the vicinity of E_F , in agreement with the refs [13,14]. The susceptibility obeys a modified Curie-Weiss behavior at elevated temperatures with an effective moment of $0.35 \mu_B$. The latter value indicates local moment behavior close to that expected for an Nb^+ ion (i.e., $4d$ configuration) and is therefore expected to be magnetic. There are several possibilities why no magnetic ordering is observed down to about 20 K. It could be that above T_c . The experimental specific-heat coefficient for Nb_3Sn corresponds to specific heat coefficient $\gamma_0= 3.2 \text{ mJ/mol K}^2$.

We computed the energy bands and Fermi surface of paramagnetic Nb_3Sn for the theoretical lattice parameters. In Figure 4 we show the band structure of paramagnetic Nb_3Sn in the vicinity of E_F for the experimental lattice constants.

The calculations reveal that there are six bands crossing along the M–X direction, which is sensitive to changes in the lattice parameters and numerical details of the calculation, as well as band dispersion about the M and X point. Changes in the latter band effectually give rise to a modification of the topology of the corresponding Fermi surface sheet for Nb_3Sn . Six bands cross the Fermi energy.

This is strong evidence in favour of gap anisotropy or different gaps on different sheets of Fermi surface. This reveals the nature of the multiple superconducting gap superconductor of Nb_3Sn . It is well known that one the conditions for multigap superconductivity to occur is that more than one band should cross the Fermi energy, which prerequisite is commonly satisfied e.g. in s-d metals.

Electronic band structure of Nb_3Sn in the vicinity of the Fermi energy is calculated with the experimental lattice parameters. The corresponding energy-band structure is shows in Figure 5. The niobium $4d$ character of the bands is highlighted by the fatness of the respective bands, proving that in spite of the quasi-gap the bands in vicinity of E_F consist mainly of $4d$ states. In our relativistic calculation the DOS of Nb_{4d} is spin-orbit split (Fig. 2). Altogether, the physical properties of Nb_3Sn are well explained by the delocalised $4d$ description. A second condition is weak interband scattering [15]. The latter is seldom met. In other hand, the electronic band structure is sensitive to structural details such as the dimerization of Nb chains (corresponding to a Γ_{12} optical phonon) and, to a much lesser extent, the tetragonal distortion ($a/c= 1.0026 \pm 0.0001$) [16, 17] or cubic ($a=b= 5.2906 \text{ \AA}$). We find the optimized crystal structure to be small distortion of the Nb sublattice.

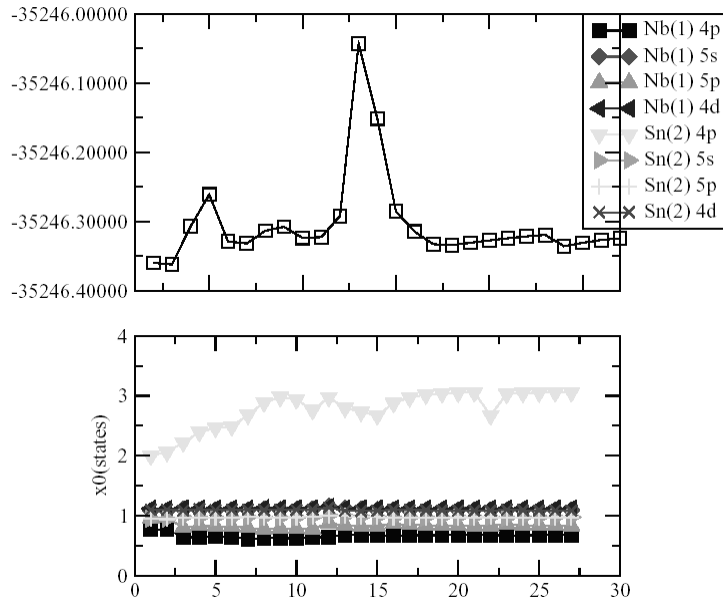


Fig. 3: Total energy in Hartree and states of Nb and Sn calculated with the theoretical Niobium positions that the hybridization is highlights.

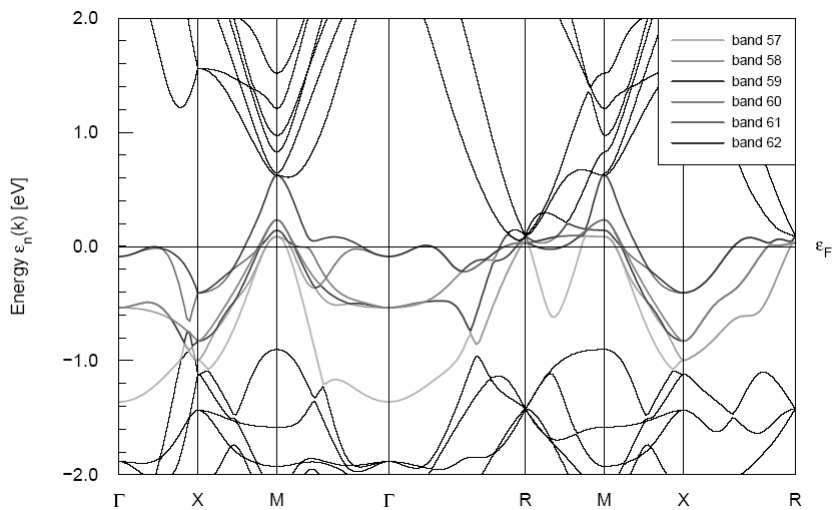


Fig. 4: (Colour online) Calculated LDA energy bands of Nb_3Sn calculated using the fully relativistic FPLO method. The bands 57, 58, 59, 60, 61 and 62 that cut the Fermi energy are highlighted by the colours.

According to the decomposition of the total DOS at the Fermi level into symmetry-projected components given by Mattheiss and Weber for the cubic phase [18] 94 % of the bare DOS originates from the Nb d-bands, in particular $d(\sigma)$ and $d(\pi)$, the remaining part being essentially due to the Nb p-band. Taking into account the large renormalization $1 + \lambda \approx 3$ for d states [4] and assuming $1 + \lambda \approx 1.2$ for the other ones, the fraction of the renormalized DOS which originates from the Nb_{4d} band becomes $\approx 92.6\%$.

This is quantitatively consistent with the experimental ratio $1 - x \approx 0.9$ [19] and given support to a scenario in which the superconducting coupling originate from the Nb d-bands, while a minor gap or several small gaps are induced in the s and p-bands by interband scattering or cooper pair tunnelling [20]. Our calculations indicate that 85% of the DOS at the Fermi energy is from the band 62 th.

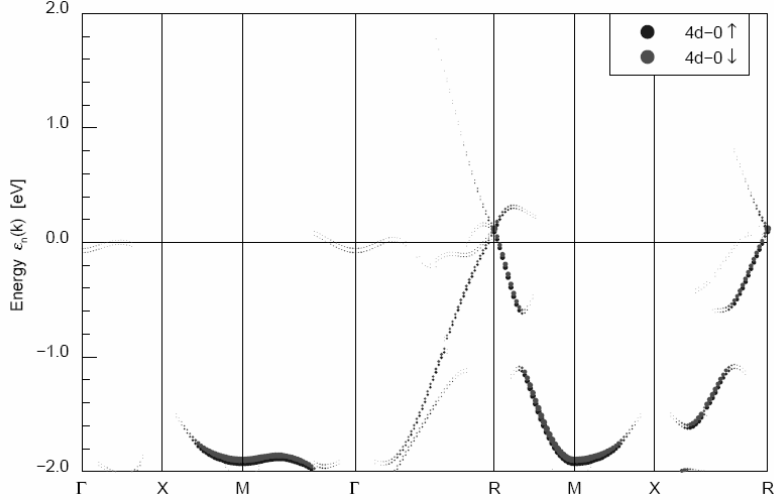


Fig. 5: The calculated LSDA energy bands of ferromagnetic Nb_3Sn in the vicinity of the Fermi level. The amount of $\text{Nb}_{4\text{d}}$ character in each of the bands is indicated by the fatness of the band.

3(b) Energy gap

The calculated gap values $2\Delta_1 = 5.67k_B T_C$ and $2\Delta_2 = 1.13k_B T_C$ above and below the BCS value

$$3.52k_B T_C \quad (1)$$

As opposed to the BCS value of 3.52, correspond to σ and π band respectively. Implies weak coupling is in error it implies that some other reason, perhaps gap anisotropy, is implicated. These results indicate weak coupling of π and can be compared with the experimental values. Now we would like to comment on the possible anisotropy of the gap. It was reported in the early tunnelling measurements of Hoffstein and Cohen that $2\Delta(0)/k_B T_c = 2.8, 2.1$ and 1.0 along $[100]$, $[110]$ and $[111]$ directions, respectively [21]. The minimum gap might be consistent with the anomaly we observe in the specific heat; the minimum other values are not.

However, more recent high quality data on superconductor/insulator/superconductor junctions exclude gap anisotropy and give $2\Delta(0)/k_B T_c = 4.1$ [22, 23]. The BCS plot of the logarithm of the specific heat versus the inverse temperature gives another way to visualize the smaller gap [2]. In Nb_3Sn , one observes a crossover from a slope higher than BCS at high temperature, to a slope -0.2 , much smaller than BCS, at low temperature. A gain, this reflects one of the gaps being larger and the other one smaller than the BCS gap, as required by the theory of two-band superconductivity [24]. Therefore, we conclude that Nb_3Sn is a new example of two-gap superconductivity.

In the spirit of Langmann [25] the s-wave clean limits of the isotropic single band (ISB), $H_{C2}(0)$ can be approximated by the formula

$$H_{C2}(0) \approx \frac{0.02T_c^2[K](1+\lambda)^{2.4}}{\nu_F^2(10^7 \text{ cm/s})} \quad (2)$$

where $\lambda = 1.8$ ($\lambda \equiv \lambda_{\text{e-ph}}$), $v_F = 0.11 \cdot 10^6$ (10^7 cm/s)

The obtained value of $H_{c2}(0)$ allows calculating the Ginzbourg-Landau parameter K, using the formula

$$K = \frac{H_{c2}(0)}{\sqrt{2}} \frac{1}{H_c(0)} \quad (3)$$

where λ , v_F and T_C are the electron-phonon coupling constant, the average Fermi velocity and the critical temperature superconductivity, respectively.

The values obtained for $H_{c2}(0)$ ($0.1 \cdot 10^{-5} T$) is negligible comparatively with that ($40 - T$) [2] given by experimental method. In this way, the obtained (GL) parameter value $K = 0.23 \cdot 10^{-5}$ is particularly small and indicates paradoxically that Nb_3Sn is a type I superconductor; it is well known that Nb_3Sn is typical type II superconductor.

3(b) Fermi surface

As basic properties of clean limit type II superconductor the upper critical field $H_{c2}(T)$ provides insight into the relationship of electronic structure, e.g. by the Fermi velocity v_F and superconductivity. The computed (FS) (Fig. 6) consists of six disjoint sheets is found to be anisotropic and to exhibit a pronounced two-dimensionality; both features prompt that a theory of superconductivity in Nb_3Sn requires a two-band approach instead of the usual isotropic, single-band model.

This is the case for bands 60 and 61 in the numbering adopted by [26], 63 th and 64 th containing the (FS) of the very flat band due to the Nb_{4d} band, assumed to be responsible for the high- T_c . The remaining candidates are mostly empty “jungle-gym” structures of holes. The calculated Fermi surface of paramagnetic Nb_3Sn is shown in Fig. 6, for the experimental lattice constants. The colors of (FS) indicate the relative sizes of Fermi velocities [(i.e., $\partial E / \partial k$)] on the sheets. A high Fermi velocity is expressed by the red color, a small Fermi velocity by the dark blue color.

There are six bands crossing E_F , giving rise to six Fermi surface sheets: A ellipse-shaped hole pocket centered at the M point, a disjoint Fermi surface portion consisting of an X centered, hole ellipsoid and one some what rectangular hole tube along the z axis. The fifth and sixth sheets are a rectangular electron tube like structure along the X–M–X edge of the Brillouin zone. The main modification of the Fermi surface with the lattice parameters occurs for the fifth Fermi sheet, which, for the theoretical lattice constants was partially open in the $z=0$ plane. Thus, this Fermi surface sheet becomes more two-dimensional for the larger lattice constants. The ab-initio calculated Fermi surface is rather simple; therefore it should not be difficult to identify the various (FS) sheets experimentally, for example in de Haas-van Alphen measurements and external orbits representation.

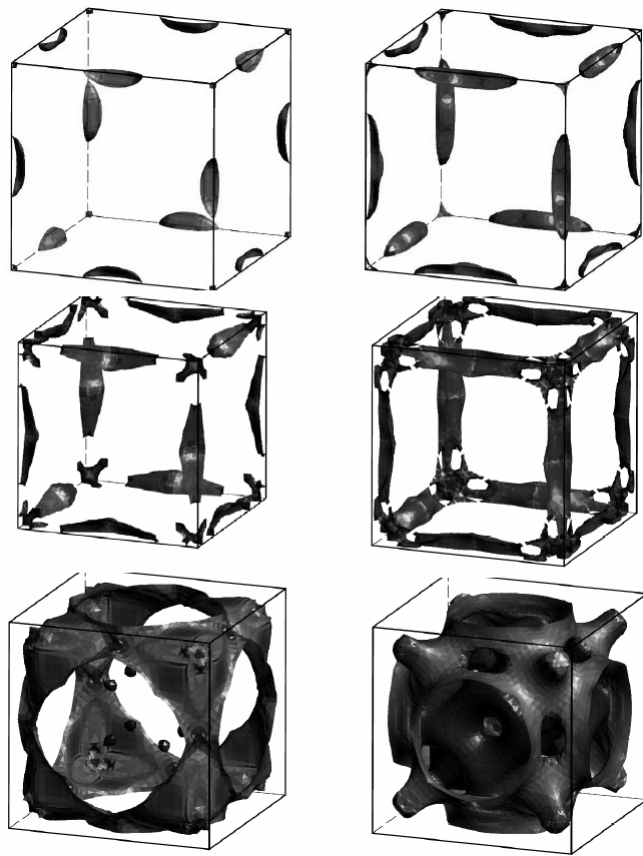


Fig. 6: (Colour online) Calculated Fermi surface of paramagnetic Nb_3Sn with external orbits for a field along the c axis indicated by the black circle. Apart from the small hole pockets at the X point and small electron at the M points, the Fermi surface sheets are pronouncedly two-dimensional. Colours depict the size of the Fermi velocity (electron and the hole velocity): blue corresponds to a small velocity, red to a large Fermi velocity. The Fermi surface sheets in the left-hand top panel correspond to band No. 57, those in the right-hand bottom panel to band No. 62.

4. Conclusion

LDA and LSDA, FPLO calculations of Nb_3Sn confirmed that the Nb_{4d} electrons controlled the superconducting properties by creation of copper-pair at E_F , and observation of the localized $4d$ electrons of Nb_3Sn emphasizes our quite reasonable understanding of electron-phonon coupling. Thus our study yields strong support for two-band superconductivity's model. The FPLO calculation indicate that about 94% of the DOS at the Fermi energy originate Nb d-band. The correct treatment of the Nb_{4d} bands is always a matter of concern, owing to the peculiar localization behaviour. The calculations assuming delocalized Nb_{4d} band predicted lattice constants that are very close. The calculation identifies the larger gap on the σ band and smaller gap on the π band where values are $5.67 \text{ k}_\text{B}T_\text{c}$ and $1.13 \text{ k}_\text{B}T_\text{c}$ above and below the BCS value $3.52 \text{ k}_\text{B}T_\text{c}$. The vortex lattice structures in cubic BCS superconductors are due to (FS) anisotropy. Our calculation is in agreement with the experiment results given in the literature.

Finally, the relationship between the upper critical field $H_{c2}(0)$ and average Fermi velocity shows that the ISB model is not valid. We find unrealistic value of $H_{c2}(0)$. In this case we conclude that the two band models superconductivity is to corresponding better. Therefore, the theory of superconductivity in Nb_3Sn requires a two-band approach instead of

the usual isotropic, single-band model. The value of the (GL) parameter K again morley below 20 confirms strongly this calculation. Explaining the superconductivity with its high T_c will certainly be a major challenge to theory in the next years.

Acknowledgements

The Author is grateful to the member of the theoretical physics group at the IFW-Dresden Germany, Drs Saad El-Gazzar and Ingo Opahle for the fortfull discussions.

References

- [1] J. Kwo, T. H. Geballe, Physica B **10** (1989)1665
- [2] J. M. Coombes, J. P. Carbotte, J. Low. Temp. Phys. **74** (1989)491
- [3] L. R. Testardi, Rev. Phys. **47** (1975) 637
- [4] J. K. Freericks, A. Y. Liu, A. Quandt, J. Greek, Phys. Rev. B **65** (2002) 224510
- [5] K. Koepernik, H. Eschrig, Phys. Rev. B **59** (1999) 1743
- [6] I. Opahle, K. Koepernik, H. Eschrig, Phys. Rev. B **60** (1999)14035
- [7] H. Eschrig, *Optimized LCAO Method and the Electronic Structure of Extended Systems*, Springer, Berlin (1989)
- [8] J. P. Perdew, A. Zunger, Phys. Rev. B **23** (1981) 5048
- [9] Z. W. Lu, B. M. Klein, Phys. Rev. Lett. **79** (1997) 1361
- [10] B. Sadigh, V. Ozolins, Phys. Rev. B **57** (1998) 2793
- [11] J. K. Freericks, Amy Y. Liu, A. Quandt, J. Geerk, arXiv: Cond-Mat. 0201048 v1 (2005)
- [12] J. M. An, W. E. Pickett, Phys. Rev. Lett. **86** (2001) 4366
- [13] J. M. An, W. E. Pickett, Phys. Rev. Lett. **86** (2001) 4366
- [14] J. Kortus, I. I. Mazin, K. D. Belashchenko, V. P. Antropov, L. L. Boyer, Phys. Rev. Lett. **86** (2001) 4656
- [15] H. Suhl, B. T. Matthias, L. R. Walter, Phys. Rev. Lett. **3** (1959)552
- [16] W. Weber, L. F. Mattheiss, Phys. Rev. B **25** (1982)2270
- [17] B. Sadigh, V. Ozolins, Phys. Rev. B **57** (1998)2793
- [18] L. F. Mattheiss, W. Weber, Phys. Rev. B **25** (1982)2248
- [19] G. Goll, Private communication (2004)
- [20] W. Weber, L. F. Mattheiss: Phys. Rev. B **37** (1988) 599
- [21] V. Hoffstein, R. W. Cohen, Phys. Rev. Lett. **29A** (1969) 603
- [22] J. K. Freerichs, A. Y. Liu, A. Quandt, J. Geerk, Phys. Rev. B **65** (2002) 224510
- [23] J. Geerk, U. Kaufmann, W. Bangert, H. Rietschell, Phys. Rev. B **33** (1986) 1621
- [24] R. combescot, Europhys. Lett. **43** (1998) 701
- [25] E. Langmann, Physica (Amsterdam) **173C** (1991) 347
- [26] L. Hoffmann, A. K. Singh, H. Takei, N. Tayota, J. Phys. F, Met. Phys. **18** (1988) 2605